Preliminary Structural Model, Teels Marsh Mineral County, Nevada

Report prepared for Dajin Resources (US) Corp.

Mark F. Coolbaugh, Ph.D., CPG

Jan. 18, 2016

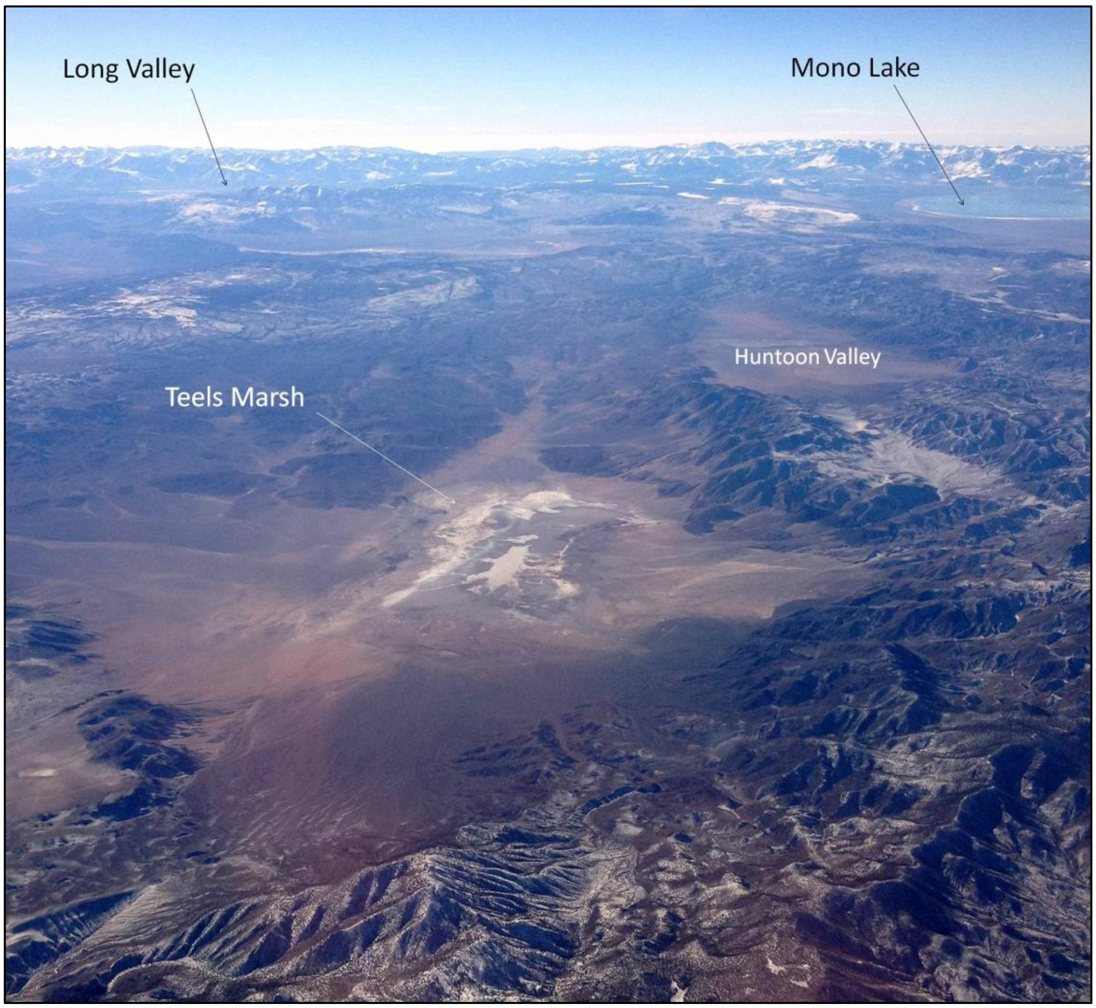

Aerial view of Teels Marsh, looking southwest, with Long Valley and Mono Lake visible in the background (photo taken from commercial airplane by the author Jan. 1, 2016).

SUMMARY

A structural model of Teels Marsh basin was constructed with the help of a detailed gravity survey and a basin-depth model derived from that survey. The structural model features a fault-bounded, northeast-trending graben 6.5-km-long and 1 to 2.4-km-wide with an estimated maximum depth (to consolidated bedrock) of greater than 2 km near the center of the basin beneath the playa. This graben is part of a structural pull-apart block in a subsiding extensional basin near the western end of the active Excelsior Mountain sinistral/normal fault zone. The graben occupies a broader, roughly circular-shaped basin 6 km in diameter. A number of secondary faults divide the basin and central graben into a series of structural blocks and sub-basins. Unconsolidated sediments within these blocks and sub-basins could be either open or closed to through-going fluid flow depending on the configuration of faults and favourable stratigraphy.

Shallow auger holes and drill-holes (<60 m) show that unconsolidated basin fill deposits include clays, clastic rocks (silts and sands), evaporite deposits, and volcanic ash (tephra). With the exception of clays, these rocks represent potential sources of permeability. Silts, sands, and conglomerates could play a greater role in defining zones of permeability at Teels Marsh than at Clayton Valley (site of active lithium production 80 km to the SE) because of the closer proximity of Teels Marsh to adjacent mountains with a steeper topographic profile. Volcanic ash beds could also host significant zones of permeability, due to the relative proximity of Teels Marsh to young volcanic centers at Mono Craters (near Mono Lake) and Long Valley, California, both located approximately 70 km to the southwest. The Bishop Tuff, which is believed to represent an important zone of permeability at Clayton Valley, is likely present in the subsurface at Teels Marsh, but depths to this ash layer are difficult to predict because depth of burial is a function of basin subsidence rates over time, and these rates are currently poorly constrained. Additional local permeability could be provided by the faults that bound the graben and sub-basins.

Introduction

A preliminary structural model of Teels Marsh represents one step in the development of a comprehensive 3D basin model. It is anticipated that the structural model, in combination with the basin depth model, will be used to help design the location of seismic surveys and initial lithium exploration drill-holes. Data from the seismic surveys and drilling can be fed back into the model to improve the resolution of fault locations, basin depths, and define stratigraphy.

No previous drilling greater than 200 feet (60 metres) in depth or seismic surveys are known to have been completed in Teels Marsh, and consequently, construction of the preliminary structural model relies on a detailed gravity survey and on constraints provided by regional tectonics and fault patterns in the region surrounding Teels Marsh.

The detailed gravity survey comprises 415 new stations measured in February and March, 2015 by Magee Geophysical Services LLC. These data were combined with regional data from 95 USGS stations; terrain corrections were applied and complete Bouguer anomalies were calculated for a range of estimated rock densities (Magee, 2015). These data were used by J. L. Wright Geophysics to generate interpretive products including a basin depth model, an elevation model of the basin bottom, and the horizontal gradient of the basin depth model (Wright, 2015). Model calculations were based on an average regional density of 2.50 g/cc and a constant density contrast between unconsolidated and consolidated rocks of 0.40 g/cc (Wright, 2015).

The style of Quaternary faulting and regional tectonic setting provide constraints for modeling structures in Teels Marsh. Fault patterns interpreted from the gravity data should be compatible, to the maximum extent possible, with the regional and local structural fabric and stress field. Published data useful in this regard include active faults mapped by Wesnousky (2005), discussions of regional faulting and tectonics (Wesnousky, 2005; Oldow et al., 2008; Ferranti et al., 2009), and the USGS Quaternary fold and fault database (U.S. Geological Survey and Nevada Bureau of Mines and Geology, 2015).

Fluid flow patterns and brine evolution in the basin are potentially influenced by the presence of thermal groundwater. The southwestern corner of Teels Marsh hosts an active but blind (no surface manifestations) geothermal system (Coolbaugh et al., 2006; Zehner et al., 2012; Coolbaugh et al., 2013), with temperatures as high as 97°C at 130 feet (40 metres) (Zehner et al., 2012). Fluid geothermometry suggests that subsurface thermal waters could attain temperatures of 150°C or higher (Coolbaugh et al., 2013). Thermal fluid flow appears controlled by some of the same faults that define basin boundaries in Teels Marsh, and the locations of upwelling thermal fluids provide information on structural permeability. Conductive heating from geothermal fluids could influence fluid flow patterns in basin sediments, as described in the Discussion section at the end of this report.

This report is accompanied by digital fault data in ArcGIS shapefile and Google Earth kmz formats, and by original digital versions of figures in the report. Supporting data in the form of digital references and GIS data are supplied to Dajin Resources on an on-going basis.

Structural Setting

Teels Marsh lies within the Walker Lane, a zone of active dextral strike-slip faults between the Sierra Nevada Mountains on the west and the Basin and Range province on the east. Strike-slip faulting in the Walker Lane is driven by the relative motions of the Pacific and North American plates; it is estimated that 20-25% of that motion is accommodated by faults in the Walker Lane instead of by the San Andreas fault system (Bennet et al., 1998). In the vicinity of Teels Marsh, the Walker Lane is characterized by subparallel ENE-striking sinistral faults and NNE- to NE-striking normal faults; this region is termed the Mina Deflection. The Mina Deflection transfers a portion of dextral strike-slip motion from the western margin of the Walker Lane northward to the eastern portion of the Walker Lane (Oldow et al., 2008; Faulds and Henry, 2008).

The Mina Deflection contains four principal ENE-striking sinistral fault systems, from north to south the Rattlesnake, Excelsior Mountain, Candelaria, and Coaldale faults (Fig. 1; Wesnousky, 2005). In most cases, these fault systems terminate on their western and eastern ends at subsidence basins that are located where the faults change from an ENE-strike to a more N- to NW-strike. Concomitant with the change in strike is a shift from sinistral motion to normal motion (Wesnousky, 2005). Basin development at the ends of these faults is driven by WNW-directed extension and/or clockwise block rotation (Wesnousky, 2005), and the relative importance of these two mechanisms has been debated (Wesnousky, 2005; Oldow et al., 2008; Ferranti et al., 2009).

Teels Marsh occupies the basin at the western mapped terminus of the Excelsior Mountain fault system (Fig. 1). As mapped by Wesnousky (2005), the Excelsior Mountain fault bounds Teels Marsh basin on its northern and western margins. On the north side of Teels Marsh, the Excelsior Mountain fault is ENE-striking and displays sinistral strike-slip motion, but the fault abruptly changes strike in the NW corner of the basin, from which it bears SWS, forming a braided system of curving normal faults, some with steep range fronts up to 500 metres high (Fig. 2). Like a left-bend or step-over in a left-lateral fault system, the NNE-striking portion of the fault system represents an extensional environment that contributed to the formation of Teels Marsh basin (Wesnousky, 2005). The NNE strike is also ideally oriented in the modern-day stress field for extension (Ferranti et al., 2009). Active geothermal systems of the Great Basin commonly form along complex portions of extensional faults. Consistent with this tendency is the presence of shallow geothermal activity at Teels Marsh focused on intersections and curving flexures of normal faults the on the west side of the Marsh (Coolbaugh et al., 2013).

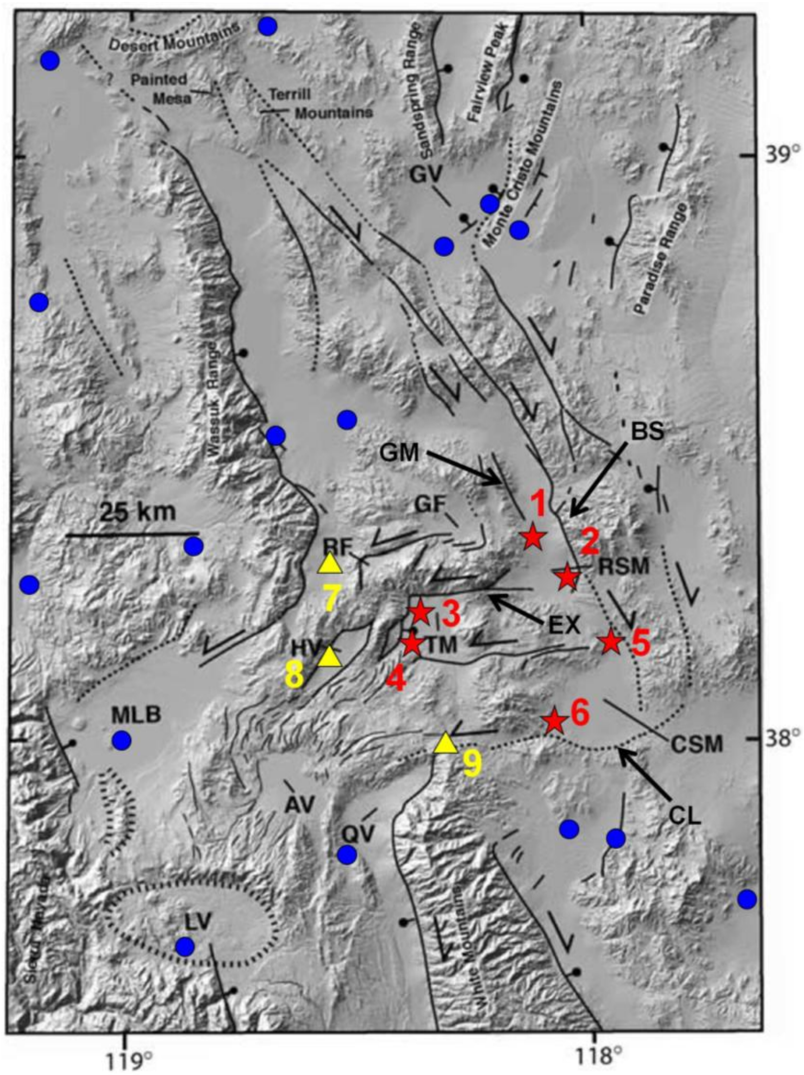

Figure 1. Quaternary faults and geothermal systems in the Mina Deflection, taken from Coolbaugh et al. (2005) and originally adapted from Wesnousky (2005). The physical extent of the Mina Deflection encompasses the geothermal areas: 1 = Sodaville, 2 = Rhodes Marsh, 3 & 4 = North & south Teels Marsh, 5 = Redlich, 6 = SW Columbus Marsh; and thermal wells 7, 8, and 9 at Whiskey Flat, Huntoon Valley, and NE of Queen Valley, respectively. RSM = Rhodes Salt Marsh, TM = Teels Marsh, CSM = Columbus Salt Marsh, GF = Garfield Flat, HV = Huntoon Valley, RF = Rattlesnake Flat, MLB = Mono Lake Basin, LV = Long Valley caldera, AV = Adobe Valley, QV = Queen Valley, GV = Gabbs Valley, EX = Excelsior Mountain fault, GM = Gumdrop Hills fault, CL = Coaldale fault, BS = Benton Springs fault. Blue circles are geothermal systems outside the Mina Deflection with measured or estimated temperatures >70°C.

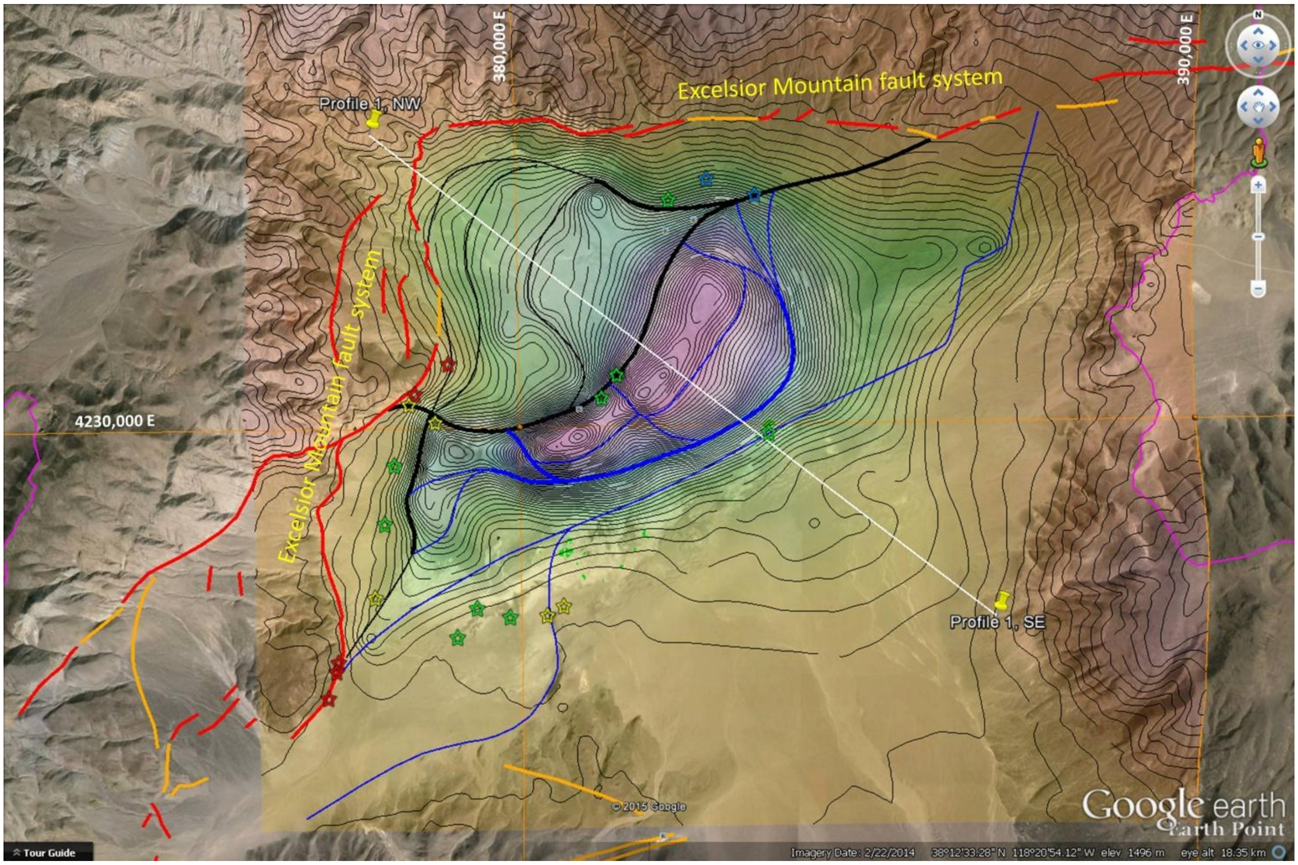

Figure 2. Structural model of Teels Marsh superimposed on Google Earth with the bottom-of-basin elevation model. Excelsior Mountain fault system of Wesnousky (2005) shown in red (known) and orange (concealed). Faults inferred from the gravity-derived basin depth model of Wright (2015) shown in black (SE-dipping) and blue (NW dipping). Thin black lines are elevation contours on the modeled elevation of the unconsolidated sediment-basement contact (prior to modeling of fault locations). Transparent shading from yellow through green and lavender represents progressively lower elevations of the unconsolidated sediment-basement contact, with lowest elevations (lavender) lying 2 to 2.5 km below surface. Colored stars depict temperatures from springs, shallow wells, and direct-push holes drilled in 2010: green <20°C, yellow 20-26°C, orange 26-37°C, red >37°C. Cross-section of Figure 4 shown with white line (profile 1). A 10-km UTM wgs84 grid is shown with thin orange lines. Magenta lines on east and west margins of image mark the 812 km^2 Teels Marsh surface catchment basin.

Geologic Setting

Pre-tertiary rocks exposed to the west, north, east, and south of Teels Marsh include shales and chert of the Ordovician Palmetto Formation, interbedded Permian volcanogenic sedimentary rocks and volcanic breccias and mafic intrusions of the Mina Formation, Triassic siltstones of the Candelaria Formation, and Mesozoic clastic sedimentary rocks of the Dunlap Formation (Garside, 1982; Stewart, 1984; Stewart et al., 1984a, 1984b). These formations are intruded on the north and west sides of Teels Marsh by plutonic rocks ranging in composition from diorite to granite (including granite of Whiskey Flat, granite of Silver Moon, granodiorite of Huntoon Valley, and diorite).

The pre-Tertiary rocks are overlain by a sequence of Oligocene to Miocene silicic tuffs comprising the Candelaria sequence (Robinson and Stewart, 1984). The tuffs are overlain in turn by andesitic volcanic rocks, which in turn are overlain by Tertiary basalts with minor intercalated tuffs and sedimentary rock including diatomite (Stewart, 1984). The Tertiary volcanics comprise the majority of surface and near-surface rocks within the catchment basin of Teels Marsh, most of which lies south of Teels Marsh. The Candelaria tuffs, because of their felsic composition, are potentially a significant source of lithium introduced to groundwater. A measured tuff section south of Teels Marsh is 150 metres thick with an unexposed base and is composed of at least 10 distinct units. The eruptive source of these tuffs is believed by Robinson and Stewart (1984) to lie in the Candelaria Hills approximately 20 to 25 km southeast of Teels Marsh.

Quaternary rocks include alluvial gravels, alluvial fan deposits, and lacustrine clays, clastics, and evaporites. Basin fill deposits in Teels Marsh, as documented in shallow auger holes (Evans, 2015) and shallow drill-hole samples (Drew, 1970; Taylor and Surdam, 1981), include variably colored, locally sulfide-bearing clay, sands, silts, evaporites, and air-fall tuff (tephra). The evaporites include sodium chloride, mined in small amounts as early as 1867 (Papke, 1976), and borax and tincalconite, which were mined from 1873 to 1892 making Teels Marsh the largest borate producer of Nevada (Papke, 1976). Water-soluble gaylussite and northupite have also been identified in shallow cores (Drew, 1970; Jones et al., 2015).

Structural Model Method/Approach

Gravity modeling (Wright, 2015) indicates that Teels Marsh is underlain by a relatively narrow, steep-sided basin up to 2.5 km deep. This fact, combined with the presence of an active fault system along the northern and western margins of the basin (the Excelsior Mountain fault), and location of Teels Marsh within the actively deforming Mina Deflection, indicates that faulting likely played a key role in basin development.

Construction of the preliminary structural model involved the following steps:

1) creation of an initial basin depth model and basin-bottom elevation model based on the detailed gravity survey (Wright, 2015),
2) identification of potential faults corresponding to elongate areas of rapid horizontal changes in basin depth and/or basin-bottom elevations, using known faults and active tectonics as constraints,
3) use of a calculated horizontal gradient of the basin depth model to enhance the visualization of rapid horizontal gradients that potentially correspond to faults (horizontal gradient image provided by Wright Geophysics),
4) use of selected vertical profiles (cross-sections) of the modeled basin-bottom elevation to better recognize overly steep gradients likely related to faulting (provided by Wright Geophysics), and,
5) creation of a representative cross-section to test fault placements and displacement magnitudes.

This preliminary model should be of the detail necessary for selection of seismic line locations and drill-hole targets. The model can be significantly refined and updated with the addition of data from the seismic profiles and drill-holes. Development of a more detailed model could be accomplished with the following steps:

6) selection of seismic lines and drill-hole targets,

7) refinement of fault locations and displacement magnitudes based on interpreted seismic sections and drilling results,
8) development of a set of cross-sections with fault placements and slip magnitudes,
9) assignment of revised basin depths in plan-view along each cross-section,
10) interpolation of basin depths and elevation of basin bottom in plan-view based on the cross-section data,
11) refinement/confirmation of the revised basin models based on the gravity signature,
12) incorporation of stratigraphic data from the seismic lines and drill-hole logs, and,
13) interpolation of the stratigraphic data using a combination of cross-sections and plan-views.

Model Results

The system of faults that comprise the structural model is illustrated in Figs. 2 through 4. Black lines denote faults with displacements down to the SE, and blue lines denote faults with displacements down to the NW. Faults marked by heavy black and blue lines have greater estimated displacements and their existence and placements are relatively certain. Faults marked by thinner black and blue lines have smaller estimated displacements and their locations are more approximate. Some of these smaller faults may not exist, and other faults of small to moderate displacement may exist but are not clearly resolvable with the gravity data.

The structural model features a prominent northeast-trending graben approximately 6.5-km-long and 1 to 2.4-km-wide that reaches a maximum estimated depth (to consolidated bedrock) beneath the playa of greater than 2 km (Figs. 2 through 4). The southeast-dipping faults (black lines of Figs. 2 and 3) form a curving system of faults that represent a reasonable and predictable extrapolation of normal faults of similar attitude that comprise the Excelsior Mountain fault system on the west side of Teels Marsh. Without the benefit of the gravity survey, a half-graben might be predicted beneath the marsh, on the basis of exposed normal faults on the west side of the marsh, and the lack of comparable faults on the east side of the marsh. However, the detailed gravity survey tells a different story. Strong gravity gradients on the SE side of the marsh argue for the existence of a NW-dipping set of faults (blue lines in Figs. 2 and 3) that combine with the SE-dipping faults to form a somewhat symmetrical, though curved in plan-view, graben. A cross-sectional view of the graben is shown in Fig. 4. The NW-dipping faults are largely concealed at the surface, though a short Quaternary fault of such orientation has been mapped at the extreme eastern margin of the basin (U.S. Geological Survey and Nevada Bureau of Mines and Geology, 2015), and the existence of a NW-dipping fault at the southwest end of the basin is suggested by topographic relationships.

The existence and location of the graben is consistent with the tectonic framework of Teels Marsh described by Wesnousky (2005). Crustal extension associated with the westward shift from strike-slip motion to normal motion along the Excelsior Mountain fault zone would naturally lead to subsidence in the form of a pull-apart block. A possible component of clockwise rotation across Teels Marsh would accentuate basin development.

Basin Stratigraphy and Permeability

Basin fill deposits beneath Teels Marsh consist of clays, silts, sands, and possible conglomerates, intercalated with ash beds and evaporite deposits. Without drilling, it is difficult to predict depths and stratigraphic positions of these units, which can be expected to vary significantly from one basin to another in Nevada and California.

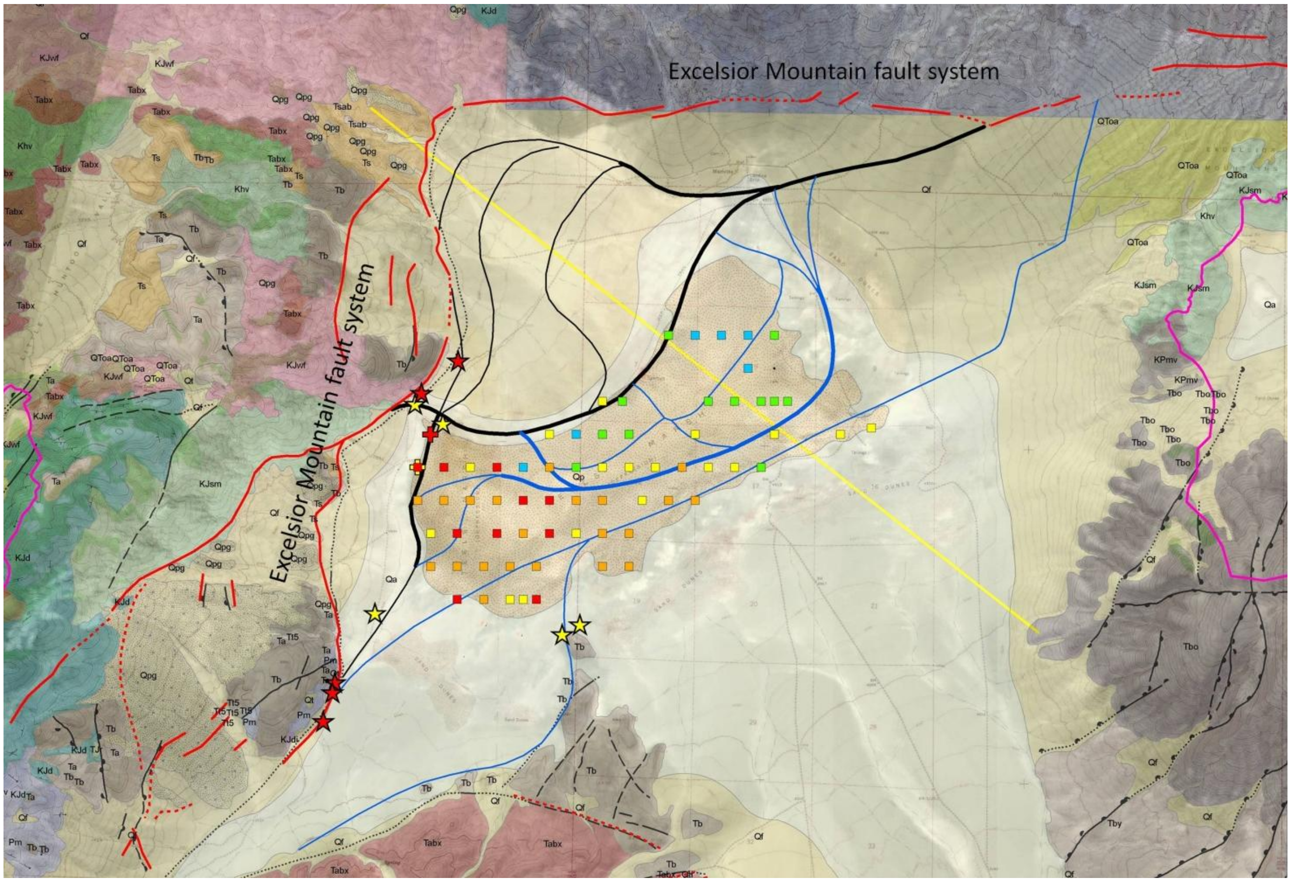

Figure 3. Structural model of Teels Marsh superimposed on 24,000-scale geology. Excelsior Mountain fault system of Wesnousky (2005) shown in solid red (known) and dotted red (concealed). Faults inferred from the gravity-derived basin depth model of Wright (2015) shown in black (SE-dipping) and blue (NW dipping). Larger displacement faults are indicated with bold black and blue lines. Colored stars depict temperatures from springs and shallow wells/geoprobe holes: yellow 20-26°C, orange 26-37°C, red >37°C. Colored squares represent maximum lithium concentrations obtained from 9-foot-deep (2.7-metre-deep) auger holes: blue 13.5-53.4 ppm, green 53.4-92.7 ppm, yellow 92.7-132.5 ppm, orange 132.5-218 ppm, red 218-460 ppm. Elevated lithium brine concentrations at two localities indicated by colored crosses: red = 70 ppm, yellow = 20 ppm. Cross-section of Figure 4 shown with straight yellow line (profile 1). Magenta lines on east and west margins of map mark the Teels Marsh surface catchment basin boundary. One-mile square section boundaries from the cadastral survey are visible as thin black lines in background. North is up.

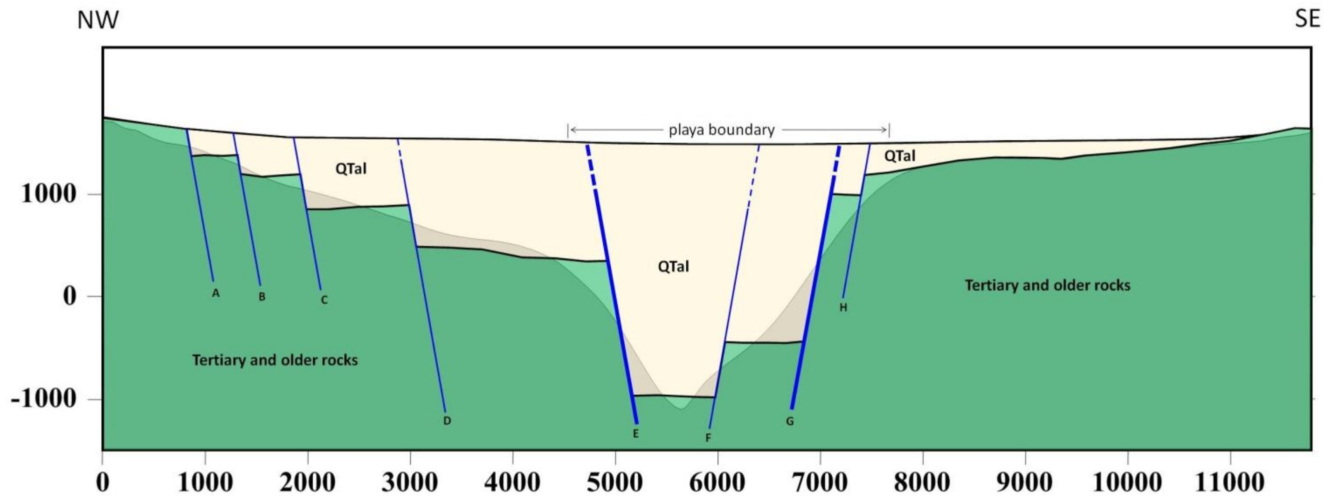

Figure 4. Cross-sectional view looking northeast of the modeled graben along profile line 1 (plan-view location shown in Figs. 2, 3). The original gravity-derived model of the basin-bottom elevation is shown with the yellow background shading. QTal = basin fill deposits, including muds, clastic rocks including silt, sand, and possible conglomerates; evaporite deposits, and ash beds (tephra layers). Tertiary and older rocks include Paleozoic and Mesozoic sedimentary and volcanic rocks, Mesozoic plutons, Tertiary volcanic rocks including basalt, andesite, probable felsic tuffs, and some Tertiary sedimentary rocks including lacustrine rocks equivalent to the Esmeralda Formation. Higher confidence is placed on faults denoted with the bold blue lines (E, G) that match strong gradients in the gravity model. Smaller faults (A-D, F, H) are known with less certainty, and in some cases, a primary sloping bedrock contact could explain the gravity model without the need for faulting. Horizontal and vertical scales are in metres, 1:1.

Potential sources of permeability in the basin include ash beds, evaporite layers, beds of relatively clean clastic material, and fault zones. Clastic beds, including conglomerates, sands and silts, could provide an important source of permeability, as exemplified by the basal fanglomerate at Clayton Valley (Zampirro, 2004). Clastic rocks could be more important for permeability at Teels Marsh than at Clayton Valley, because distances to erosional highlands are less at Teels Marsh and the topographic gradient is higher. In the South American altiplano, similar 'immature' basins tend to have a significant component of clastic-hosted permeability (Houston et al., 2011).

Ash beds (tephra layers) are an important contributor to permeability in the Clayton Valley brine field 80 km to the southeast (Davis et al., 1986; Zampirro, 2004), and they are likely to be important at Teels Marsh as well. Both basins are located east of volcanic eruptive centers at Long Valley and Mono Craters, California. Clayton Valley is located 100 km due east of Long Valley and 120 km ESE of Mono Craters, whereas Teels Marsh is located 70 km NE from both eruptive centers (see photo on title page of this report). Hay (1964) reports at least eight "vitric rhyolitic" tuffs ranging up to 5 inches (13 cm) thick at depths of 1 to 16 feet (0.3 to 5 metres) in auger holes sampled up to 20 feet (6 metres) deep at Teels Marsh. Taylor and Surdam (1981) similarly report ash beds in shallow holes up to 40 feet deep. The ash beds are variably altered to a mineral assemblage that includes calcite and the zeolite minerals phillipsite, analcime, clinoptilolite, and chabazite (Hay, 1964; Drew, 1970; Taylor and Surdam, 1981; Jones et al., 2015). Searlesite and dolomite have also been identified in the tuffaceous sediments and muds (Drew, 1970; Taylor and Surdam, 1981; Jones et al., 2015).

Additional and potentially thicker air-fall tuffs are likely to occur at depths below the shallow auger drilling at Teels Marsh. At Clayton Valley, the 5- to 30-foot-thick (1.5 to 9.1 metres) "Main Ash Aquifer" occurs at depths of 200 to 750 feet (60 to 230 metres), and an additional system of permeable ash beds (the "Lower Aquifer System") lies below the Main Ash Aquifer (Zampirro, 2004). The Main Ash Aquifer has been tentatively correlated by Zampirro (2004) to the 0.76 m.a. Bishop Tuff erupted from the Long Valley caldera.

The depths to equivalent tuffs at Teels Marsh are poorly constrained, but because maximum basin depths at Teels Marsh are greater than at Clayton Valley, the depths to similarly aged tephras could also be greater. Oldow et al. (2008) place the onset of extensional faulting in the western part of the Mina Deflection at 3 m.a. If subsidence at Teels Marsh began 3 m.y. ago and continued at a constant rate to the present, the Bishop Tuff would lay at approximately 1/4 the total depth of the basin at any given location. However, subsidence rates are likely to have shifted with time, making it difficult (without drilling) to accurately determine the depth to the Bishop Tuff or to other regionally correlated tephras. At Clayton Valley, the depth to the Main Ash Aquifer is roughly 2/3rds the total basin depth. Relative depths to the Bishop Tuff in Teels Marsh and Clayton Valley are likely to be different because Clayton Valley lies outside the Mina Deflection and is therefore likely to have experienced a different subsidence rate history.

Evaporite horizons dominated by sodium chloride are also potential sources of permeability. Salt is an important constituent of core samples from shallow auger holes (Jones et al., 2015), and it is likely to be present at greater depths, though permeability may be expected to decrease with depth.

Finally, the faults themselves represent zones of potential structurally derived permeability, especially given the active tectonic setting of Teels Marsh. Even at Clayton Valley, where tectonism is less active, faulting is locally associated with permeability, in some cases allowing the transmission of dilute external fluids into the basin and in other cases allowing for interbasin flow (Davis et al., 1986). Of course, faults also impede permeability and trap heavy brines in localized portions of basins (Zampirro, 2004; Houston et al., 2011).

Discussion

Elevated concentrations of lithium in shallow (0 to 2.7 metre) sediments (130-460 ppm) and brines (up to 70 ppm) occur in the SW portion of Teels Marsh (Fig. 3). Basin depths are relatively shallow there, but geothermal activity surrounds the area of anomalism on three sides (Fig. 3). In contrast, shallow sediments and brines overlying the deepest portion of the graben farther to the NE have lower lithium concentrations (typically less than 90 ppm for sediments), although sediment lithium concentrations increase to over 130 ppm at depths greater than 15-20 metres, based on limited geoprobe sampling. Leaching by encroaching dilute groundwater might explain the lower near-surface lithium sediment concentrations in the northern area, but the SW area lies at essentially the same elevation and may receive a similar, if not greater, influx of dilute groundwater based on the location of drainages and presence of springs. Convection of brines in the sub-surface offers a possible alternative explanation. Such convection could be driven by conductive heating of basin brines by geothermal fluids, and facilitated by possible permeability along basin faults and favourable stratigraphy. Convection of brines has been noted at some of the South American lithium-bearing salares (Houston et al., 2011). If such convection is occurring at Teels Marsh, it provides evidence of possible elevated lithium brine concentrations at depth and evidence of through-going permeability within the basin, even if significant portions of the basin may not be participating in such basin-scale flow.

Recommendations

The preliminary structural model reveals a deep, fault-bounded graben set within a broader, more circular basin. The distribution of near-surface lithium concentrations points to possible subsurface brine circulation, but if such flow is occurring, it is likely that not all portions of the basin participate in that flow (i.e., sub-surface compartmentalization of fluids may present). Compartmentalization is made possible by faults and stratigraphic aquicludes that form barriers to fluid flow and trap evolved brines with elevated lithium contents, as at Clayton Valley (Zampirro, 2004). For this reason, exploratory drilling should test multiple structural blocks.

Seismic surveys can improve the accuracy and resolution of the structural model. Without specific knowledge of fault locations, the definition of structural blocks provided by the detailed gravity survey is approximate. Multiple interpretations of the gravity model in terms of fault locations and displacement magnitudes are possible, especially for smaller faults, which although having small displacements can still exercise significant control on sub-surface brine accumulation, as per Clayton Valley (Zampirro, 2004). The seismic profiles can also delineate potentially permeable stratigraphic units. The depth to reflection horizons can guide initial drill planning, and they can be used to predict depths to aquifers after the first few holes have been drilled.

Finally, lithium-bearing brines with concentrations of up to 70 ppm were encountered in two shallow auger holes in the extreme NW end of the playa. A follow-up shallow auger sampling program could help refine the distribution of these brines and lead to a better understanding how they formed and what type of basin fluid flow system they might be related to.

The locations of four proposed seismic lines (Fig. 5) have benefitted from input from Leonard Harrand of Eagle Exploration Inc and Jerry Schwinkendorf. Three of the lines are designed to respectively cross three sub-basins at nearly right angles near the centers of the respective sub-basins. The NE line has been extended northwestward to evaluate possible basin sediments NW of the deep graben. The fourth seismic line follows the axis of the graben, with the object of better defining the location of cross-faults that are presumed to control the location of sub-basins in the graben.

Ten proposed exploratory drill sites are shown in Fig. 5. These sites have been selected to test as many structural blocks as possible, while still providing good coverage of the basin as a whole. Two of the proposed sites are on adjacent property to the east and permission is being sought to drill these wells.

The selection of drill depths is influenced by multiple factors. Due to compaction and temperature increases, permeability will generally decrease with depth, and pumping costs will increase. However, the decrease in permeability with depth is more gradual for clastic materials than it is for salt (Houston et al., 2011), which is a point in favor of relatively deep drilling at Teels Marsh, given the immature nature of the basin and expected relative abundance of clastic material. Little is known about the presence of deeper lithium brine aquifers in other closed basins around the world, because most production comes from very shallow aquifers (<50 metres) and limited deep drilling data are available (Houston et al., 2011; Kesler et al., 2012). The deepest current brine production in the world comes from Clayton Valley, where production wells were up to 250 metres (820 feet) deep in 1986 (Davis et al., 1986).

One of the more important aquifers at Clayton Valley is the "Main Ash Aquifer", correlated by Zampirro et al. (2004) with the 0.76 Ma Bishop Tuff. As discussed in the previous section on 'Basin Stratigraphy and Permeability', the Bishop Tuff is almost certainly present at Teels Marsh, but depths to the aquifer are poorly constrained. If subsidence rates were constant over the last 3 m.y., depth to the Bishop Tuff might be approximately ¼ the modeled depth of the basin sediments (see section on 'Basin Stratigraphy and Permeability'). If this is the case, depth to the Bishop Tuff would be approximately 1,000 feet (300 metres) in the relatively shallow southwestern basin targeted by drill-hole 1, and approximately 1,800 feet (560 metres) in the deeper sub-basin targeted by drill-hole 2 (Fig. 5). These depths could be used as minimum total depths for some of the initial drill-holes. An argument could be made for selective testing of deeper horizons where clastic units such as fanglomerates might be present. In any case, prior to finalizing target depths, it will be important to use the seismic profiles to help identify potentially permeable horizons at specific drill-hole locations.

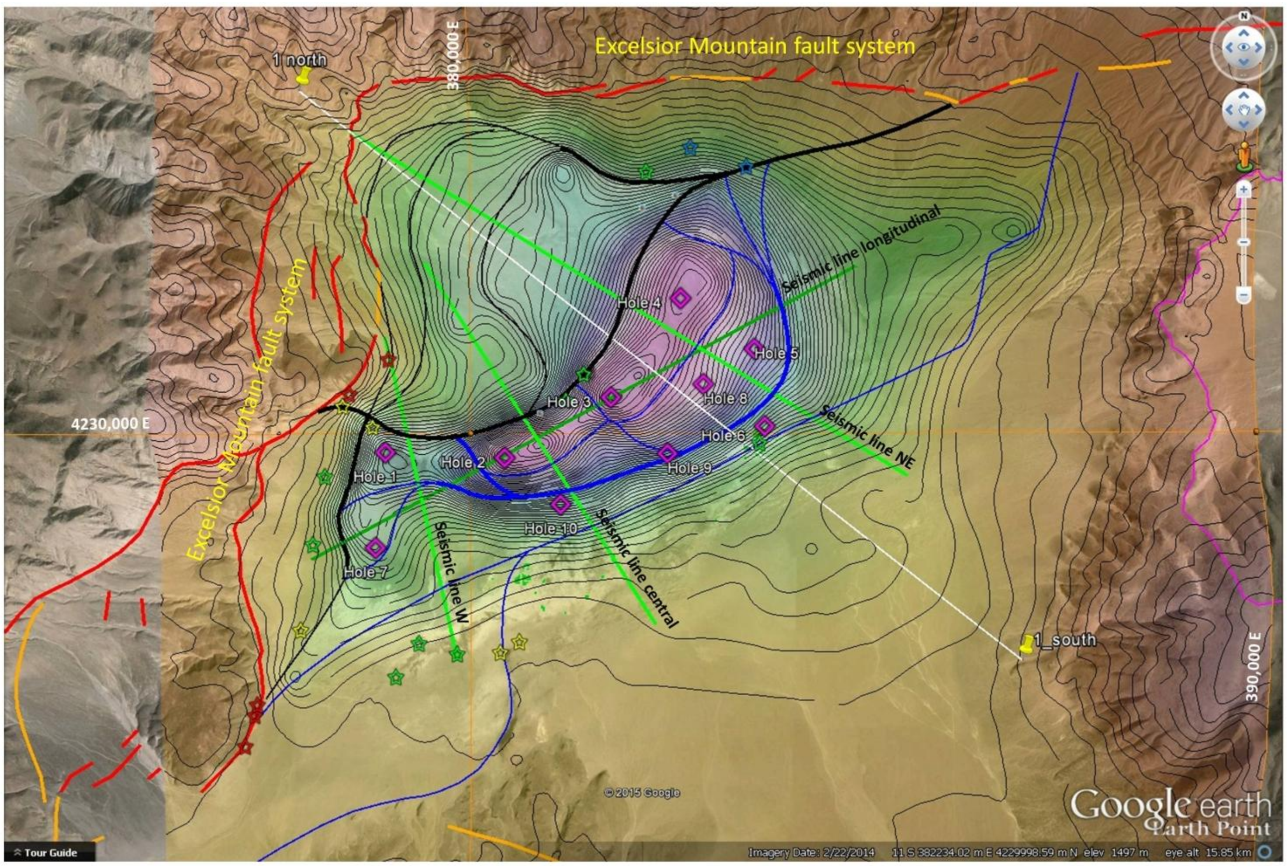

Figure 5. Location of recommended seismic lines and exploratory drill-holes. Drill-holes are symbolized with magenta diamonds. See Fig. 2 for explanation of colored lines (faults, catchment boundary, coordinate grid, cross-section trace, and basin bottom contours), as well as for background color shading (basin bottom elevation), and colored stars (spring and well temperatures).

References

Bennett, R.A., Wernicke, B.P., and Davis, J.L., 1998, Continuous GPS measurements of contemporary deformation across the northern Basin and Range province, Geophysical Research Letters, v. 25, p. 563-566.

Coolbaugh, M.F., Kratt, C., Sladek, C., Zehner, R.E., and Shevenell, L., 2006, Quaternary borate deposits as a geothermal exploration tool in the Great Basin: Geothermal Resources Council Transactions, v. 30, p. 393-398.

Coolbaugh, M., Kratt, C., Faulds, J., Zehner, R., and Sladek, C., 2013, Active geothermal systems of the Mina Deflection, southwestern Nevada, *in* L.J. Garside, ed., Geothermal and Petroleum Developments in Several Extensional Basins of the Central Walker Lane, Nevada: 2013 Nevada Petroleum and Geothermal Society Field Trip Guidebook, Oct. 12-13, 2013, p. 101-116.

Davis, J.R., Friedman, I., and Gleason, J.D., 1986, Origin of the lithium-rich brine, Clayton Valley, Nevada: U.S. Geological Survey Bulletin 1622, 138 p.

Drew, P., 1970, Geochemistry of iron and clay mineralogy of playa sediments from Teels Marsh, Nevada: M.A. thesis, University of Wisconsin, Madison, Wisconsin, 69 p.

Evans, T.L. Jr., 2015, Sediment and brine auger sampling at Teels Marsh playa, Mineral County, Nevada: report prepared for Dajin Resources Corp. June 22, 2015, 5 p.

Faulds, J.E., and Henry, C.D., 2008, Tectonic influences on the spatial and temporal evolution of the Walker Lane: An incipient transform fault along the evolving Pacific – North American plate boundary, *in* Spencer, J.E., and Titley, S.R., eds., Circum-Pacific Tectonics, Geologic Evolution, and Ore Deposits: Tucson, Arizona Geological Society, Digest 22, p. 437-470.

Ferranti, L., Oldow, J.S., Geissman, J.W., and Nell, M.M., 2009, Flattening strain during coordinated slip on a curved fault array, Rhodes Salt Marsh extensional basin, central Walker Lane, west-central Nevada, *in* Oldow, J.S., and Cashman, P.H., eds., Late Cenozoic Structure and Evolution of the Great Basin–Sierra Nevada Transition: Geological Society of America Special Paper 447, p. 189–213.

Garside, L.J., 1982, Geologic map of the Moho Mountain quadrangle, Nevada: Nevada Bureau of Mines and Geology Map 74.

Hay, R.L., 1964, Phillipsite of saline lakes and soils; American Mineralogist, v. 49, p. 1366-1387.

Houston, J., Butcher, A., Ehren, P., Evans, K., and Godfrey, L., 2011, The evaluation of brine prospects and the requirement for modifications to filing standards; Economic Geology, v. 106, p. 1225-1239.

Jones, C.G., Carlson, C.T., and Moore, J.N., 2015, X-ray diffraction analyses of 15 sediment core samples from Teels Marsh, NV: Energy and Geoscience Institute report for Dajin Resources, October, 2015, 22 p.

Kesler, S.E., Gruber, P.W., Medina, P.A., Keoleian, G.A., Everson, M.P., and Wallington, T.J., 2012, Global lithium resources: relative importance of pegmatite, brine and other deposits; Ore Geology Reviews, v. 48, p. 55-69.

Magee Geophysical Services, 2015, Gravity survey over the Teels Marsh prospect, Mineral County, NV; consulting report submitted to Dajin Resources (US) Corp., March, 2015, 5 p.

Oldow, J.S., Geissman, J.W., and Stockli, D.F., 2008, Evolution and strain reorganization within Late Neogene structural stopovers linking the central Walker Lane and northern Eastern California Shear Zone, western Great Basin: International Geology Review, v. 50, p. 270-290.

Papke, K.G., 1976, Evaporites and brines in Nevada playas; Nevada Bureau of Mines and Geology Bulletin 87, 35 p.

Robinson, P.T. and Stewart, J.H., 1984, Uppermost Oligocene and lowermost Miocene ash-flow tuffs of western Nevada: U.S. Geological Survey Bulletin 1557, 53 p.

Stewart, J.H., 1984, Geologic map of the Teels Marsh quadrangle, Mineral County, Nevada: U.S. Geological Survey Open-File Report OF-84-504.

Stewart, J.H., Kleinhampl, F.J., and Johannesen, D.C., 1984a, Geologic map of the Rattlesnake Flat quadrangle, Mineral County, Nevada: U.S. Geological Survey Open-File Report OF-84-506.

Stewart, J.H., Kleinhampl, F.J., Speed, R.C., and Johannesen, D.C., 1984b, Geologic map of the Little Huntoon Valley quadrangle, Mineral County, Nevada: U.S. Geological Survey Open-File Report OF-84-503.

Taylor, M.W. and Surdam, R.C., 1981, Zeolite reactions in the tuffaceous sediments at Teels Marsh, Nevada; Clays and Clay Minerals, v. 29, n. 5, p. 341-352.

U.S. Geological Survey and Nevada Bureau of Mines and Geology, 2015, Quaternary fault and fold database for the United States, accessed Jan. 28, 2015, from USGS web site: http//earthquakes.usgs.gov/regional/qfaults/.

Wesnousky, S.G., 2005, Active faulting in the Walker Lane: Tectonics, v. 24, 35 p.

Wright, J.L., 2015, Teels Marsh Property gravity and airborne magnetic surveys: basin model and GIS compilation; consulting report submitted to Dajin Resources Corp., March 11, 2015, 30 p.

Zampirro, D., 2004, Hydrogeology of Clayton Valley brine deposits, Esmeralda County, Nevada, *in* Castor, S.B., Papke, K.G., and Meeuwig, R.O., eds., Betting on industrial minerals: Proceedings of the 39th Forum on the Geology of Industrial Minerals, Reno-Sparks, Nevada, May 18-24, 2003; Nevada Bureau of Mines and Geology Special Publication 33, p. 271-280.

Zehner, R.E., Tullar, K.N., and Rutledge, E., 2012, Effectiveness of 2-meter and geoprobe shallow temperature surveys in early stage geothermal exploration: Geothermal Resources Council Transactions, v. 36, p. 835-841.